

Some Characteristics of the Martian Aphelion Global Cloud Belt. M. J. Wolff¹, R. T. Clancy¹, B. A. Whitney¹, P. R. Christensen², and J. C. Pearl³, ¹Space Science Institute (1540 30th Street, Suite 23, Boulder CO 80303-1012; wolff@colorado.edu), ²Arizona State University, ³NASA/Goddard Space Flight Center

Introduction: The presence of discrete condensate clouds on Mars is certainly not a new discovery, having been observed through most of the documented history of telescopic monitoring [1]. Furthermore, spacecraft data have been used to study discrete cloud features in the Martian atmosphere in greater detail, *e.g.*, morphology, seasonal occurrence [2,3,4]. Condensate clouds, specifically discrete water ice clouds, appeared to be regarded as fairly common but, with the possible exception of the polar regions, generally uninteresting from a climatological point of view [5]. However, recent observations indicate that in addition to their large spatial scale, the water ice clouds may in fact play a more prominent role in the Martian climate.

Microwave monitoring of global atmospheric temperature profiles since 1982 indicates that the lower 50 km of the Martian atmosphere is generally 15-20 K cooler in the northern spring (aphelion) and summer seasons than has generally been reported for the Viking period [6]. While recent work reveals that part of the difference in the higher altitudes sampled by the 15 micron channel of the Viking Infrared Thermal Mapper (25 km) may be due to a "surface leak" in that bandpass [7], the temperatures at the lower altitudes (<20 km) cannot be similarly reconciled. Such low temperatures lead to saturation of global water vapor above 5--10 km (versus above 20--25 km during the Viking period [8]) and the conditions necessary for globally extant water ice cloud formation. General circulation models predict a cross-equatorial Hadley cell during the northern spring/summer season [9]. With the observed water saturation altitudes, water ice clouds would be expected to form in the ascending branch of this circulation north of the equator [4]. Such a global-scale cloud belt has not been identified in the Viking era data, although efforts to reexamine the Viking data set are under way [10]. However, an example of such a structure is noted by Slipher [11], and it has been detected repeatedly by the Hubble Space Telescope (HST) during the past several Martian apparitions [6,12,13], see Figure 1. The presence of these cloud formations provides for dynamic, nonlinear interactions with the Martian atmosphere, in particular with airborne dust particles, on both short and long time-scales[6].

In this paper, we wish to examine the spatial and temporal variations of the cloud belt optical depth, as well as the microphysical characteristics of the water ice particles themselves.

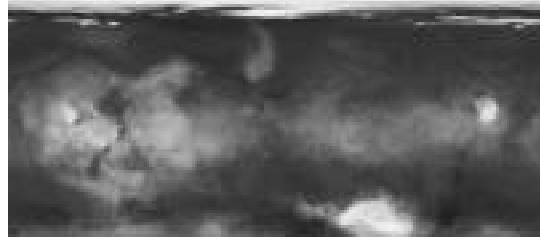


Figure 1: Aphelion global cloud belt in March 1997 seen by HST at 410 nm.

Cloud Optical Depths: As part of a synoptic monitoring program, we have obtained a panchromatic set of images which span the period from 1990-1999 (though we are presenting only data from the period 1992-1997). The data were taken by both the Planetary Camera and the Wide Field Planetary Camera 2, and were reduced/calibrating using standard techniques (see [13] and references within for more detail). Due to the need for contrast between dust and water ice particles (as well as with the surface), we focus our analysis on the 410 and 502 nm images. Optical depths for each component were retrieved using a multiple scattering radiative transfer code which, along with the parameters employed, is described in [13].

Our primary goal in the analysis is to quantify the seasonal variability of the equatorial cloud belt. Using the images as a guide, we restrict our analysis to the range of latitudes bounded by -20° and $+40^\circ$. In this region, we examine several subsections for each observational epoch. Thus, we are able also to characterize diurnal effects (see Figure 2). The relative differences of the cloud and dust albedos as a function of wavelength allow one to discriminate well between the effects of water ice clouds and dust. In practice, the generally low-to-moderate levels of dust we find make it problematic to quantify the small perturbations which might be expected from spatial variations, where we define "small" as being less than our uncertainties (typically $\sim 0.1-0.2$). We adopt the use of an "average" optical depth value to characterize the diffuse dust loading in the equatorial region.

The water ice cloud opacities do show similar trends across all three of the seasons sampled by HST. In particular, we identify three facets of our analysis which bear specific mention:

1. We observe a clear correlation between the formation of the global equatorial cloud belt with season: the initial onset of the formation of the water ice cloud belt is near aphelion ($L_S \sim 70^\circ$), and the largest optical depths occur at $L_S = 60^\circ-100^\circ$.

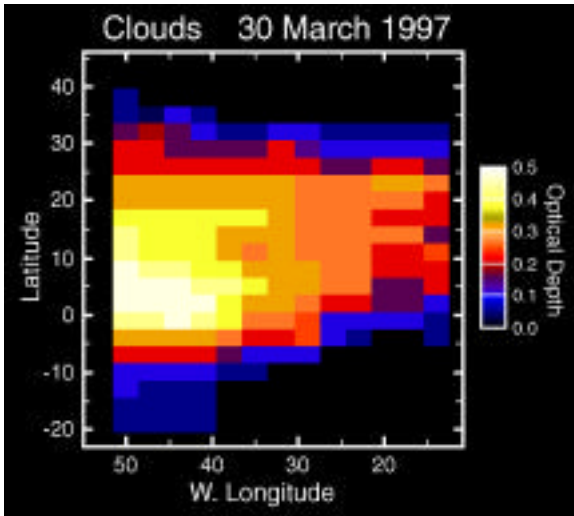


Figure 2: Optical Depth as a function of latitude and local time (~9:00 am left, ~12:00 -right), March 1997.

As discussed by [6], this can be understood at a basic level through the large variation in solar insolation between aphelion and perihelion (~40%). The altitude of water ice cloud formation, as characterized by water vapor saturation, is a function of the atmospheric thermal structure. Reduced solar flux, resulting in cooler temperatures, lowers the altitude of water ice cloud formation. Under the assumption of uniform water and dust vertical distributions, lower clouds simply have more water from which to form and condensation nuclei around which to do so.

2. We find that the clouds are concentrated between the latitudes of -10° and $+30^\circ$ and that the peak opacity occurs generally at a point offset to the north of the equator. [6] argues that the observed water ice cloud belt is being formed in the advecting (*i.e.*, northern) branch of the cell. The water ice clouds form in the upward advecting branch, possibly impeding the flow of water to the south. However, one cannot rule out the possibility that the water ice is transported by the Hadley cell without detailed calculations. The northern boundary and the peak cloud opacity of the observed cloud band correlates well with the global character of the Hadley cell modeled near aphelion (*i.e.*, [9, 14]).

3. The equatorial water ice cloud belt tends to disappear with the approach of the equinox ($L_S=180^\circ$). This would also be expected if the water ice cloud formation is being driven by the Hadley cell, which weakens and transitions into two relatively weak cells [14]. While the seasonal distribution of the data in this paper is not well sampled near the equinox, the trend is clear nonetheless.

Microphysical Properties: This aspect of our work is in progress. We intend to present radiative transfer/electromagnetic scattering analyses employing both bolometer and spectrograph data from the Ther-

mal Emission Spectrograph onboard the Mars Global Surveyor; *e.g.*, [15]. Our goal is to constrain both the size distribution of the water ice aerosols (and to a lesser degree, the dust particles) and the particle topology (*i.e.*, shape; composition, allowing for mixtures of ice and dust). The former task focuses on the visible-to-infrared opacity ratio (using nadir and limb views), while the latter utilizes the emission phase function (EPF) sequences. In order to maximize the signal of the clouds, we restrict spatial and temporal coverage to that which coincides with the global cloud belt.

Our scattering algorithms allow for multiple shapes, including cylinders, hexagonal prisms, and spheroids. Explicit treatment of mixed compositions of ice and dust are being examined using both approximate (*e.g.*, multi-layer spheres) and finite element techniques (*e.g.*, discrete dipole approximation). Our radiative transfer codes include plane-parallel “layer” and discrete ordinates. In addition, we have developed a monte carlo transfer model in order to accurately treat the case of limb.

References: [1] Martin et al. (1992) in *Mars*, 34-70. [2] Smith and Smith (1972) *Icaurs*, 16, 509-521. [3] French et al. (1981) *Icarus*, 45, 468-493. [4] Kahn (1984) *JGR*, 89, 6671-6688. [5] Jakosky and Haberle (1992) in *Mars*, 969-1016. [6] Clancy et al. (1996) *Icarus*, 122, 36-62. [7] Wilson and Richardson (1999) *JGR*, in review. [8] Jacquin et al. (1986) *Icarus*, 68, 442-461. [9] Haberle et al. (1993) *JGR*, 98, 3093-3123. [10] Tamppari et al. (1996) *Bull. Amer. Astron. Soc.* 29, 961. [11] Slipher (1962) *Photographic Story of Mars*. [12] James et al. (1996) *JGR*, 101, 18,883-18,890. [13] Wolff et al. (1999) *JGR*, 104, 9027-9041. [14] Zurek (1992) in *Mars*, 799-817. [15] Christensen et al. (1998) *Science*, 278, 1758-1768.